

# Inverse Relationship Between the Intraretinal Concentration of Bioavailable Nitric Oxide and Blood Glucose in Early Experimental Diabetic Retinopathy

Micah J. Guthrie, Christian R. Osswald, and Jennifer J. Kang-Mieler

Department of Biomedical Engineering, Illinois Institute of Technology, Chicago, Illinois, United States

Correspondence: Jennifer J. Kang-Mieler, Department of Biomedical Engineering, Illinois Institute of Technology, 3255 South Dearborn Street, Wishnick Hall, Room 314, Chicago, IL 60616, USA; jkangmie@iit.edu.

Submitted: September 29, 2014  
Accepted: November 25, 2014

Citation: Guthrie MJ, Osswald CR, Kang-Mieler JJ. Inverse relationship between the intraretinal concentration of bioavailable nitric oxide and blood glucose in early experimental diabetic retinopathy. *Invest Ophthalmol Vis Sci.* 2015;56:37-44. DOI:10.1167/iovs.14-15777

**PURPOSE.** To directly measure in vivo retinal nitric oxide (NO) concentration in experimental early diabetic retinopathy and correlate measurements with blood glucose to determine how intraretinal NO changes with severity of diabetes.

**METHODS.** Long-Evans rats were made diabetic with streptozotocin (STZ). Three weeks post STZ injection, intraretinal NO concentration profiles were recorded using a dual NO/electroretinogram microelectrode. Diabetic profiles were compared with profiles from healthy controls, healthy rats injected with the NO synthase inhibitor L-NG-nitroarginine methyl ester (L-NAME), and healthy rats that received acute glucose injections (“acute hyperglycemia”). The NO values at the retina/RPE boundary (100% retinal depth) and retinal surface (0% depth) were analyzed for correlation with blood glucose.

**RESULTS.** The average NO concentrations in the outer retina, inner retina, and vitreous humor of mild diabetic rats (250–400 mg/dL) were significantly higher than controls by 73%, 47%, and 70%, respectively. The average NO concentrations in the outer retina, inner retina, and vitreous humor of severe diabetic rats (500–600 mg/dL) were lower than controls, with NO at 41%, 36%, and 36% of controls, respectively, similar to L-NAME-treated eyes (38%, 36%, 20% of control). The NO levels in moderate diabetic rats (400–500 mg/dL) and acute hyperglycemia rats were similar to controls. The NO was significantly and inversely correlated with blood glucose for diabetic rats at 100% depth ( $R = -0.91$ ) and 0% depth ( $R = -0.79$ ) but not for acute hyperglycemia rats.

**CONCLUSIONS.** The higher-than-control level of NO in mild diabetic rats and lower-than-control level in severe diabetic rats show that severity of diabetes is an important factor when measuring the bioavailability of NO in diabetic retinopathy.

Keywords: nitric oxide, diabetic retinopathy, intraretinal electrode

The development of diabetic retinopathy (DR) has been associated with nitric oxide (NO). Increased plasma levels of NO (as determined from plasma nitrite and nitrate) have been found in diabetic patients with retinopathy compared with diabetic individuals without retinopathy or healthy controls.<sup>1,2</sup> Diabetic retinopathy is divided into two stages: an early, nonproliferative stage and a late, proliferative stage. The nonproliferative stage is characterized by the development of microvascular abnormalities and edema resulting from the breakdown of the blood-retina barrier. The breakdown of the blood-retina barrier is one of the earliest events in DR, and NO has been shown to play a role in catalyzing the breakdown.<sup>3-5</sup> Therefore, it is important to characterize the changes in NO in early DR.

Nitric oxide has been shown to be modulated early on in experimental DR.<sup>6,7</sup> Although there is agreement that NO levels change in early experimental DR, the literature is conflicted as to whether the levels increase or decrease. Nitrite and nitrate levels (used as indicators of NO production) in diabetic rodent retinas have been reported to both increase<sup>3,7</sup> and decrease<sup>8</sup> at similar time points in early DR. A study by Patel et al.<sup>9</sup> found that although the levels of nitrite plus nitrate (which indicate the amount of total NO

production) increased in diabetic rat retinas, the level of nitrite (which alone is an indicator of the amount of bioavailable NO) decreased, a finding that was further supported by decreased fluorescence of a fluorescent NO indicator in the diabetic retinas. Given that nitrate formation is favored in the presence of superoxide,<sup>10</sup> the values obtained from nitrate/nitrite analyses indicate relative levels of total NO rather than bioavailable NO.<sup>11</sup> This means that a nitrate/nitrite analysis could imply that NO is increasing while the actual tissue environment is experiencing a subnormal level of NO.

Fluorescent probes, such as the diaminofluorescein (DAF) family of probes, provide clearer information about bioavailable NO; however, they do not allow for correlation of fluorescence with the actual concentration of NO unless coupled with in situ measurements from an NO microelectrode.<sup>12</sup> Changes in NO during the development of DR can have severe consequences, with overproduction leading to cytotoxicity, neurodegeneration, vascular dysfunction, and apoptosis,<sup>13</sup> and underproduction leading to an impairment of normal physiological function.<sup>14</sup> Thus, it is critical that the NO concentration in early stages of DR be directly measured to determine the bioavailability of NO.

Additionally, the vast majority of these studies did not correlate their measurements with the blood glucose level of the test animal. Instead, animals are often placed into one overall diabetic group regardless of their severity of hyperglycemia. It has been reported that NO production in certain cells is correlated with blood glucose.<sup>15</sup> Therefore, it is important to measure blood glucose along with the concentration of bioavailable NO and determine if there is any correlation between the severity of diabetes and NO.

In this study, direct measurements of intraretinal NO concentration were made with a dual NO/ERG electrode that has been described previously.<sup>16</sup> The measurements from this dual NO/ERG electrode provide a direct NO concentration measurement within the retina. The study used control rats and streptozotocin (STZ)-induced diabetic rats at 3 weeks after induction. The 3-week time point was chosen because the breakdown of the blood-retina barrier and increased NO have been detected in STZ-induced diabetic rats as early as 2 weeks post STZ.<sup>3,17</sup> Additionally, preliminary studies in our laboratory have found significant changes in retinal blood flow at 3 weeks in STZ-induced diabetic rats (Turturro SB, unpublished data, 2011). Blood glucose was measured immediately after NO measurement and correlated with NO measurements. The broad-spectrum nitric oxide synthase (NOS) inhibitor, L-NG-nitroarginine methyl ester (L-NAME), was injected into the vitreous humor of healthy rats to serve as a positive control. To test whether the NO changes seen in DR were a direct effect of exposure to high glucose, intraretinal NO was also measured from a group of healthy rats that received acute injections of glucose to maintain elevated blood glucose. Dark-adapted ERGs also were assessed to determine the effects of changes in NO on retinal function.

## MATERIALS AND METHODS

### Diabetic Rat Model

All animal procedures were performed in accordance with protocols approved by the Institutional Animal Care and Use Committee at the Illinois Institute of Technology, and with the principles embodied in the Statement on the Use of Animals in Ophthalmic and Vision Research adopted by the Association for Research in Vision and Ophthalmology. Male Long-Evans rats (325–375 g; Harlan Laboratories, Indianapolis, IN, USA) were injected intraperitoneally with a single dose of 80 mg STZ/kg body weight (BW) (Sigma-Aldrich Corp., St. Louis, MO, USA) in 2 mL/kg BW 0.09 M citrate buffer (pH 4.0). Blood glucose levels were measured using a handheld glucose meter (TRUEtrack; Walgreen Co., Deerfield, IL, USA) preinjection and weekly thereafter for 3 weeks from blood collected via the tail vein. Rats with blood glucose lower than 250 mg/dL at any time point were excluded from the study. Body weight was monitored weekly. No animals received insulin treatment.

### Electrode Fabrication and Calibration

Electrodes were fabricated as described previously.<sup>16</sup> Briefly, double-barreled theta capillary glass with one barrel containing a 5- $\mu$ m-diameter carbon fiber was heated and pulled to a fine tip (8–10  $\mu$ m). The carbon fiber served as the NO sensor and the empty barrel containing an Ag/AgCl wire served as the voltage-sensing barrel for ERG measurement as well as the reference for the NO sensor. The tip was beveled to a sharp angle and the carbon fiber electrochemically etched to create a recess. The recess was filled with a Nafion membrane to repel anionic molecules, such as ascorbic acid and nitrite.<sup>18</sup> Nitric oxide was measured amperometrically in a two-electrode

configuration at +0.9 V held between the working carbon fiber electrode and reference electrode. Nitric oxide was oxidized at the carbon fiber surface, resulting in the generation of a small redox current that was measured by a potentiostat (DY2011; Digi-Ivy, Austin, TX, USA). The oxidized NO was then rapidly converted into nitrite in aqueous media.<sup>18</sup>

The electrodes were calibrated as described previously.<sup>16</sup> Electrodes underwent a two-point calibration using NO released from the decomposition of diethylammonium (Z)-1-(N,N-diethylamino)diazen-1-ium-1,2-diolate (DEA/NO) (Cayman Chemicals, Ann Arbor, MI, USA). At 37°C in air-equilibrated PBS, 2.0 and 5.6  $\mu$ M DEA/NO released maximum levels of 0.99 and 2.19  $\mu$ M NO, respectively.<sup>19</sup> The electrodes had an average sensitivity for NO of approximately 0.9  $\mu$ M/pA and a selectivity of more than 2000:1 for NO:ascorbate and 6:1 for NO:dopamine, with an average detection limit of 0.25  $\mu$ M NO.<sup>16</sup>

### In Vivo Eyecup Preparation

The NO measurements were made from an in vivo eyecup preparation that was still attached to the living animal and perfused by the systemic vasculature. The cornea and lens were removed to make room for the electrodes due to the large volume that the lens occupies in the rat eye. Rats were initially anesthetized by 3% isoflurane in an air mixture that contained 30% oxygen, first through a mask and then a tracheal tube after tracheotomy. The femoral vein was cannulated and bolus injections of urethane (10% wt/vol, 0.25 mL) were administered every 20 minutes until the loading dose (400 mg/kg BW) was achieved. After the loading dose was reached, a bolus injection of the muscle-paralyzing agent pancuronium bromide (0.8 mg/kg BW) was administered and the animal placed on artificial respiration. Urethane (20 mg/kg BW/h) and pancuronium bromide (0.4 mg/kg BW/h) were administered continuously via syringe pump throughout the experiment to maintain deep anesthesia. The animals' heart rates and oxygen saturations were monitored by a pulse oximeter and their body temperatures maintained at 37°C using a heating pad.

The in vivo eyecup was prepared by first excising the eyelids to prevent interference. The conjunctiva was then removed with small scissors to expose the sclera and eye muscles. The eye muscles were cut to prevent them from exerting any traction on the eye. Care was taken to avoid severing the vortex veins during eye muscle removal to prevent choroidal effusion. A long-chain cyanoacrylate glue (Gluture; Abbott Laboratories, Abbott Park, IL, USA) used for wound closure in veterinary procedures was then applied from below the equatorial region of the eye up to the corneal border around the circumference of the eye. Once hardened, the glue supported the eye wall and maintained its normal contours. An incision was made at the corneal border with a scalpel blade and micro-scissors were then used to remove the cornea. The lens was then carefully extracted from the eye with toothed forceps. Most of the vitreous was usually removed along with lens. The eyecup was then filled with Ames' media (pH 7.4) to maintain the health of the retina.

### Electroretinography and NO Depth Profiles

The intraretinal ERG was recorded from the voltage barrel of the electrode and referenced to a silver subdermal electrode on the animal's head. The ERGs were elicited with full-field Ganzfeld stimulation at a flash intensity of 307 scotopic cd\*s/m<sup>2</sup> and flash duration of approximately 2 ms. The ERGs were amplified ( $\times$ 1000, ADA400A; Tektronix, Addison, IL, USA), filtered (low pass, 3 kHz), digitized (10 kHz), and stored on a computer. Animals were dark-adapted for a minimum of 1 hour

TABLE. Blood Glucose and BW of Diabetic Rats Over 3 Weeks

	Blood Glucose, mg/dL				Weight, g			
	Pre-STZ	1 wk	2 wk	3 wk	Pre-STZ	1 wk	2 wk	3 wk
Mild DR	132 ± 5	381 ± 30	384 ± 25	344 ± 13	364 ± 19	339 ± 16	315 ± 15	305 ± 13
Moderate DR	145 ± 3	412 ± 32	384 ± 28	447 ± 18	347 ± 18	292 ± 16	262 ± 15	250 ± 18
Severe DR	129 ± 11	389 ± 35	460 ± 31	541 ± 13	328 ± 27	271 ± 25	246 ± 24	242 ± 22

before the recording of ERGs. Both ERG and NO measurements were made inside an enclosed Faraday cage to decrease noise and block light. The NO measurements were made under the same dark-adapted conditions as the ERGs.

To create a depth profile of retinal NO concentration, the retina was first penetrated while recording intraretinal ERGs to determine the location of the various retinal layers. The electrode was advanced slowly toward the retina with a motorized micropositioner (MX1641R; Siskiyou, Grants Pass, OR, USA). Penetration of the retinal surface was indicated by a sharp transient in the voltage trace on the oscilloscope (due to a piezoelectric effect) and a reverse in polarity of the ERG. The micropositioner was zeroed at the surface and advanced in steps of 30  $\mu\text{m}$ , with ERGs being recorded at each step. The electrode was advanced until the RPE was reached, indicated by a voltage drop and/or pulsation of the voltage trace on the oscilloscope. The track length from the retinal surface to the RPE was then used to calculate percent retinal depth, with the retinal surface being 0% and the RPE being 100%. Once the RPE was reached, the NO electrode was polarized to +0.9 V and the current allowed to stabilize. The electrode was then withdrawn at a rate of 1.5  $\mu\text{m}/\text{s}$  while recording the current and stopped when the electrode was 200  $\mu\text{m}$  away (into the vitreous humor) from the retinal surface.

The sensitivity of the electrode was used to convert the current recording into NO concentration and the NO concentration was then plotted with the corresponding percent retinal depth to create a NO depth profile of the retina. Each data point in the profile occurred at a slightly different depth compared with another profile due to the variability of the track lengths and angles of penetration. To make a standard profile for averaging purposes, values from each profile were interpolated to fit a standard profile with points at every 2.5% depth from 0% to 100%. The standard profiles were then averaged together for each group.

### Experiment Groups

Diabetic rats were divided into three groups based on the severity of their hyperglycemia at the time the NO profiles were recorded: "mild diabetic rats" (250–400 mg/dL,  $n = 7$ ), "moderate diabetic rats" (400–500 mg/dL,  $n = 4$ ), and "severe diabetic rats" (500–600 mg/dL,  $n = 4$ ). In addition to the diabetic rats, control NO measurements were made in healthy, untreated rats ( $n = 6$ ). A broad-spectrum NOS inhibitor, L-NAME, was injected into the vitreous humor of these healthy rats after the untreated control profiles were recorded to achieve an approximate vitreal concentration of 5 mM. These L-NAME measurements served as a positive control ("L-NAME treated").

To determine the extent that high glucose levels affect NO production, another group of healthy rats ( $n = 6$ ) was injected intravenously with a bolus of 0.6 mL of 40% D-glucose solution ("acute hyperglycemia"). The glucose solution was then continuously infused (1.0–2.5 mL/h) to achieve the desired blood glucose level for a minimum of 3 hours before the recording of NO profiles. To match the diabetic rats, these

acute hyperglycemia rats were divided into three groups based on their blood glucose level.

### Statistics

Nitric oxide and ERG values for all groups were compared using one-way ANOVA ( $\alpha = 0.05$ ) with the Holm-Sidak post hoc test. Significance is achieved in the Holm-Sidak test if the adjusted  $P$  value is less than the critical value. Correlation between NO values and blood glucose was analyzed with the Pearson product-moment correlation coefficient ( $\alpha = 0.05$ ). To simplify the statistical analysis of the average profiles, the data from the standard profiles were averaged into bins. The outer retina bin included 100% to 60% depth, the inner retina bin included 57.5% to 0%, and the vitreous humor bin included  $-2.5\%$  to  $-50\%$ . All averages are presented as mean  $\pm$  SEM and all error bars in figures represent SEM.

### RESULTS

The average weekly weight and blood glucose values for the diabetic rats over the 3-week period are shown in the Table. All diabetic rats lost weight over the duration of the study and exhibited polyuria. All diabetic animals had elevated ( $>250$  mg/dL) blood glucose at 1 week post STZ and maintained elevated levels until the end of the study. Blood glucose levels for every animal in all experimental groups were monitored during the NO measurement experiments to ensure that surgical procedures did not induce any unintended changes in blood glucose. No significant alterations in blood glucose were observed due to any experimental procedure (other than acute glucose infusion).

### Intraretinal NO Concentration

The average NO profiles for the diabetic rats recorded at 3 weeks post STZ injection can be seen in Figure 1A and the average acute hyperglycemia profiles in Figure 1B. The average control profiles showed higher levels of NO in the region of the photoreceptors than in the inner retina and vitreous humor and are consistent with previous NO profiles recorded from healthy rat retinas.<sup>16</sup> The diabetic profiles were different from controls and the differences varied depending on the severity of diabetes. The mild diabetic profiles showed an increase in NO in all areas of the retina compared with the control profiles, particularly in the photoreceptor region. The moderate diabetic profiles were similar to controls. Severe diabetic profiles showed a significant reduction in NO compared with controls. Furthermore, severe diabetic profiles were similar to the L-NAME-treated profiles, suggesting that NO production in the severe diabetic rats was possibly impaired. None of the average acute hyperglycemic profiles showed any differences from controls (Fig. 1B).

For purposes of statistical comparison, values from the NO profiles were grouped into bins to detect any spatial differences in the profiles between groups. The outer retina bin (100%–60% depth; Fig. 2A) for control had an average NO concentration of

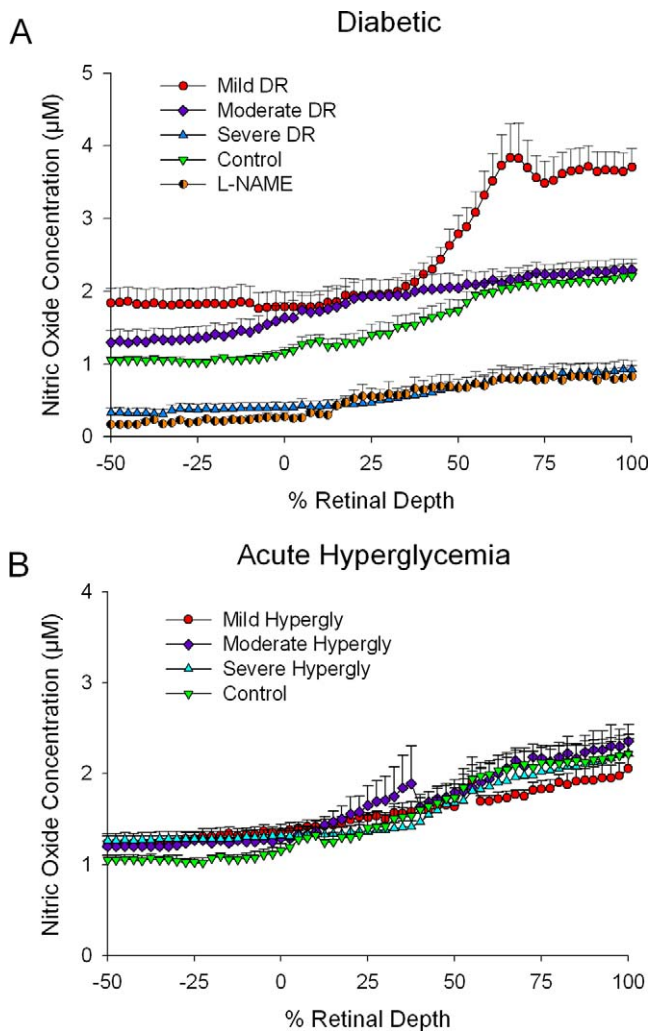


**FIGURE 1.** Average NO profiles for diabetic rats at 3 weeks post STZ injection and for acute hyperglycemia rats: 100% retinal depth corresponds to the RPE boundary, 0% to the retinal surface, and negative values to the vitreous humor. (A) Average NO profiles for mild DR, moderate DR, severe DR, control, and L-NAME groups. (B) Average profiles for mild acute hyperglycemia, moderate acute hyperglycemia, severe acute hyperglycemia, and control rats.

2.12 ± 0.17 µM. The average NO concentration in the outer retina of mild diabetic rats was significantly higher than controls by 73% (3.65 ± 0.30 µM;  $P = 7 \times 10^{-6}$ , critical level = 0.01). The outer retina NO concentration was significantly lower in severe diabetic rats with NO at 41% of control (0.86 ± 0.12 µM;  $P = 4 \times 10^{-4}$ , critical level = 0.01) and in L-NAME-treated eyes with NO at 38% of control (0.81 ± 0.16 µM;  $P = 3 \times 10^{-3}$ , critical value = 0.01). There was no difference between controls and moderate diabetic rats nor any of the acute hyperglycemia groups.

The inner retina bin (57.5%–0% depth; Fig. 2B) for controls had an average NO concentration of 1.48 ± 0.11 µM. The inner retina NO concentration was significantly higher in mild diabetic rats by 47% (2.18 ± 0.19 µM;  $P = 1 \times 10^{-3}$ , critical level = 0.01). The inner retina NO concentration was significantly lower in severe diabetic rats with NO at 36% of controls (0.54 ± 0.09 µM;  $P = 6 \times 10^{-6}$ , critical level = 0.01) and in L-NAME-treated eyes with NO also at 36% of controls (0.53 ± 0.09 µM;  $P = 9 \times 10^{-4}$ , critical value = 0.01). There was no difference between controls and moderate diabetic rats nor any of the acute hyperglycemia groups.

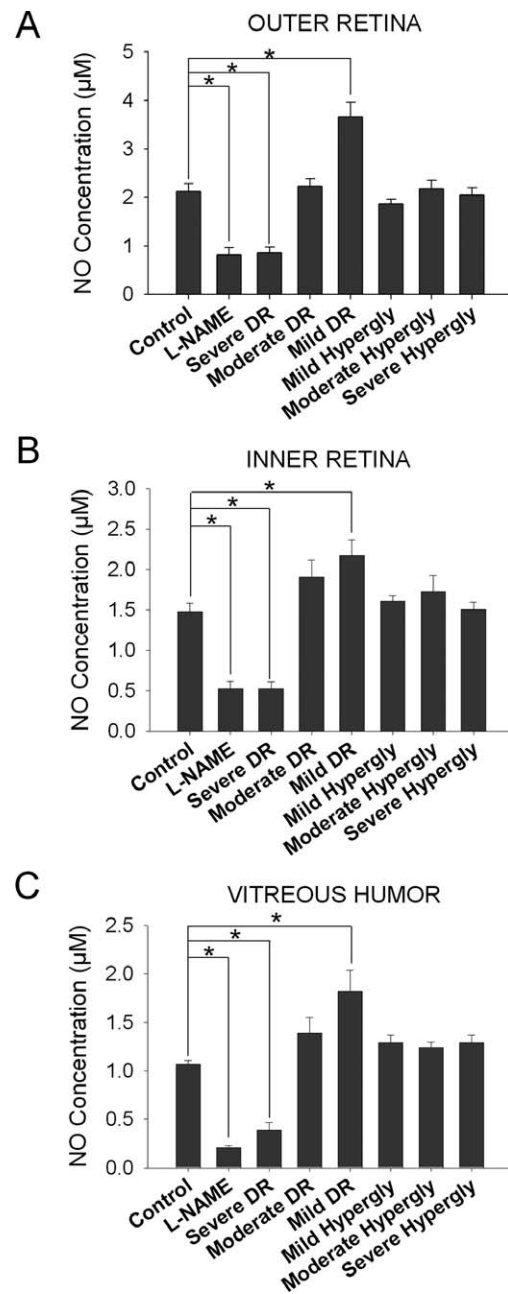


**FIGURE 2.** Average in NO concentration for NO profiles from all groups. (A) Outer retina bin, 100% to 60% depth. (B) Inner retina bin, 57.5% to 0% depth. (C) Vitreous humor, -2.5% to -50% depth. Asterisk indicates significant difference versus control.

The vitreous humor bin (-2.5% to -50% depth; Fig. 2C) for controls had an average NO concentration of 1.07 ± 0.04 µM. The NO concentration in the vitreous humor of mild diabetic rats was significantly higher than controls by 70% (1.82 ± 0.22 µM;  $P = 6 \times 10^{-4}$ , critical level = 0.01). The vitreous humor NO concentration was lower in severe diabetic rats with NO at 36% of controls (0.39 ± 0.08 µM;  $P = 4 \times 10^{-4}$ , critical level = 0.01) and in L-NAME-treated eyes with NO at 20% of controls (0.21 ± 0.03 µM;  $P = 3 \times 10^{-4}$ , critical value = 0.01), respectively. There was no difference between controls nor moderate diabetic rats nor any of the acute hyperglycemia groups.

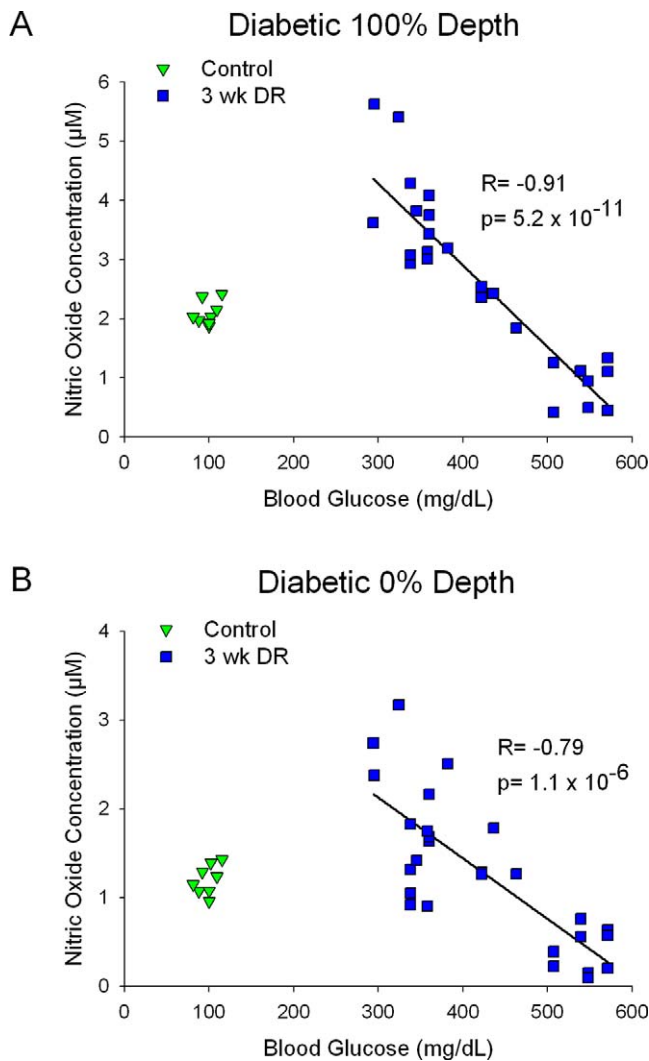


**FIGURE 3.** Nitric oxide versus blood glucose for control and diabetic rats at 3 weeks post STZ. (A) Nitric oxide versus blood glucose at 100% retinal depth. (B) Nitric oxide versus blood glucose at 0% retinal depth. The Pearson product-moment correlation coefficient (*R*) and *P* value are shown for significant correlations.

### Intraretinal NO Versus Blood Glucose

To determine the correlation between NO and blood glucose, the NO values for diabetic rats at 100% depth and 0% depth at 3 weeks were examined against the blood glucose values measured concurrently (Fig. 3). The control group showed no significant correlation between NO and blood glucose at either depth. However, the diabetic rats showed a significant correlation at 100% depth ( $R = -0.91$ ,  $P = 5.2 \times 10^{-11}$ ) and 0% depth ( $R = -0.79$ ,  $P = 1.1 \times 10^{-6}$ ), with NO being higher than control for mild diabetic rats and lower for severe diabetic rats. The correlation at 100% depth was stronger than at 0% depth.

To determine if this correlation was a direct result of exposure to high glucose, the NO and blood glucose values for the acute hyperglycemia rats also were examined for correlation (Fig. 4). Similar to lack of changes in the NO profiles of acute hyperglycemia rats, there were no significant correlations between NO and blood glucose from acute hyperglycemia ( $P \geq 0.57$ ).

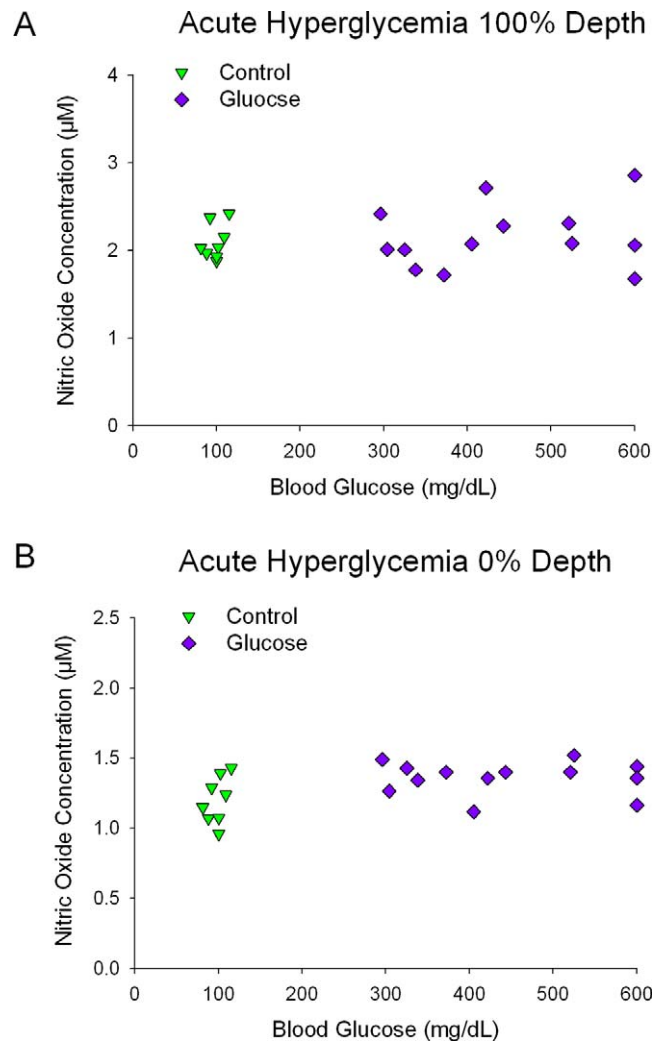


**FIGURE 4.** Nitric oxide versus blood glucose for control and acute hyperglycemia rats. (A) Nitric oxide versus blood glucose at 100% retinal depth. (B) Nitric oxide versus blood glucose at 0% retinal depth. There were no significant correlations.

### Electroretinography

The average maximum dark-adapted a- and b-wave amplitudes from each depth profile for all groups are shown in Figure 5. The average dark-adapted maximum control a-wave was  $125 \pm 10 \mu\text{V}$  and the b-wave was  $678 \pm 40 \mu\text{V}$ . The mild diabetic a-wave amplitudes were significantly higher than controls by 58% ( $197.8 \pm 23.6 \mu\text{V}$ ;  $P = 3 \times 10^{-3}$ , critical value =  $7 \times 10^{-3}$ ). The moderate diabetic a-wave amplitudes were not significantly different from the control. The severe diabetic and L-NAME a-wave amplitudes were significantly lower than controls with severe diabetic a-waves at 42% the amplitude of controls ( $52.0 \pm 15.2 \mu\text{V}$ ;  $P = 6 \times 10^{-3}$ , critical value =  $9 \times 10^{-3}$ ) and L-NAME a-wave amplitudes at 46% ( $57.6 \pm 20.8 \mu\text{V}$ ;  $P = 1 \times 10^{-2}$ , critical value =  $1.01 \times 10^{-2}$ ). The mild diabetic b-wave amplitudes were significantly higher than controls by 28% ( $866.0 \pm 46.42 \mu\text{V}$ ;  $P = 6 \times 10^{-3}$ , critical value =  $9 \times 10^{-3}$ ). Severe diabetic b-waves were 53% ( $360.3 \pm 15.6 \mu\text{V}$ ;  $P = 6 \times 10^{-5}$ , critical value =  $7 \times 10^{-3}$ ) of control amplitudes and L-NAME b-waves were 70.7% of mild diabetic rats ( $479.2 \pm 100.32 \mu\text{V}$ ;  $P = 6 \times 10^{-3}$ , critical value = 0.01). Moderate diabetic b-waves were not significantly different from controls ( $788.6 \pm 55.4 \mu\text{V}$ ;  $P = 0.15$ , critical value = 0.01).

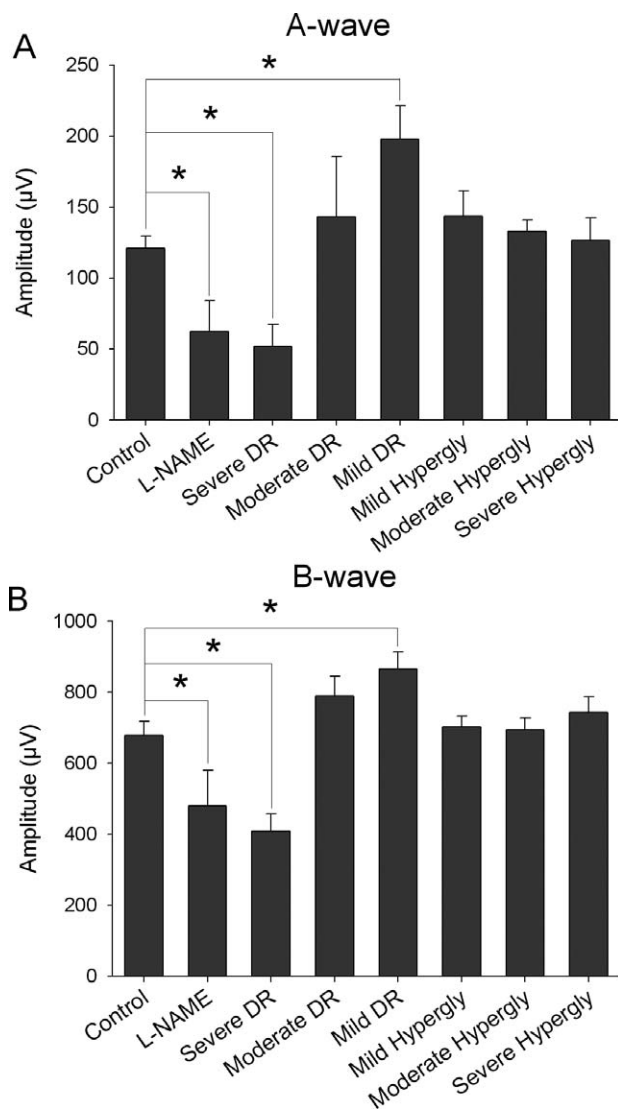


**FIGURE 5.** Maximum dark-adapted intraretinal ERG amplitudes for all groups. (A) Maximum a-wave. (B) Maximum b-wave. Severe diabetic and L-NAME a- and b-wave amplitudes were significantly lower than control, whereas moderate diabetic a- and b-wave amplitudes were significantly higher. Asterisk indicates significant difference.

## DISCUSSION

To our knowledge, this is the first study to measure the direct concentration of intraretinal NO in diabetic animals. The current study examined the NO concentration at three different levels of severity of diabetes at an early stage of the disease and compared the diabetic rats with healthy controls. Control NO profiles had high NO levels near the RPE and photoreceptors and localized regions of increased NO in the inner retina at the amacrine/ganglion cell layer. This corresponds with what is known about NO sources in the normal rat retina and is consistent with our previous work.<sup>16</sup> Vielma et al.<sup>20</sup> used fluorophore DAF-2 to stain for NO in rat retina slices and observed significant amounts of NO in the RPE and photoreceptor inner segments and the amacrine and ganglion cells in the inner retina, with no significant NO production in the middle of the rat retina near the bipolar cells. Localized regions of increased NO of approximately 100 to 400 nM, possibly originating from the amacrine or ganglion cells, were occasionally observed in the amacrine/ganglion cell layer of

control profiles, as in previous work,<sup>16</sup> and in the mild diabetic and acute hyperglycemia profiles; however, these localized increases cannot be seen in the average profiles (Fig. 2A), as they were averaged out due to their location varying from 0% to 30% depth.

Mild diabetic animals showed 73% higher levels of NO compared with controls in the outer retina where the photoreceptors are located. The photoreceptors of STZ-induced diabetic rats show high levels of oxidative stress<sup>21</sup> and morphological changes to the photoreceptors are one of the first major changes in the retinas of STZ-induced rats, occurring between 1 and 4 weeks after induction.<sup>22–24</sup> The high levels of oxidative stress in the photoreceptors may have caused high NO production as a result of neuronal nitric oxide synthase (nNOS) activation.<sup>6,25</sup> A limitation of the current measurement technique is that it is not possible to distinguish from which NOS isoforms the NO was produced. However, in future studies the contributions of the different isoforms may be isolated through the use of specific NOS inhibitors.<sup>26</sup>

Severe diabetic rats, in contrast to mild diabetic rats, had greatly decreased levels of NO compared with controls in all areas of the retina (36%–41% of controls). Similarity of the severe DR NO profile to the L-NAME treated profiles suggests a significant decrease in NO production. It is possible that the significant decrease in NO may be due to dysfunction in NOS activity, perhaps with NOS being uncoupled so that it produces superoxide instead of NO.<sup>27</sup> Another possible explanation for the decrease in NO concentration is that NO was rapidly consumed by reacting with superoxide to form peroxynitrite.<sup>3</sup> Nitric oxide production could still have been elevated in severe diabetic rats but it is possible that NO may have been consumed before it could have an effect in the surrounding tissue or be recorded by the electrode.

Moderate diabetic NO profiles did not show any significant differences from controls, although the NO level in the inner retina of moderate diabetic rats tended to be higher than controls. It is possible that the mechanisms that decreased NO in the severe diabetic rats were only partially active in the moderate diabetic rats, perhaps because the levels of superoxide or peroxynitrite were not high enough to suppress NO levels as thoroughly as in the severe diabetic rats.

The differences in NO between the levels of diabetic severity are supported by their corresponding ERGs. Nitric oxide donors have been reported to increase the amplitude of the ERG<sup>28,29</sup> as well as the light responses of individual photoreceptors.<sup>29</sup> The NOS inhibitors and NO scavengers have been shown to cause a decrease in ERG amplitude.<sup>29,30</sup> Previous studies in our laboratory also have shown that the NO donor S-nitroso-N-acetylpenicillamine increases the amplitude of the a- and b-waves in dark-adapted corneal ERGs of rats and that L-NAME decreases the amplitudes (Biol G., et al. *IOVS* 2004;45:ARVO E-Abstract 2593). It is thought that NO affects the ERG primarily through an increase in cyclic guanosine monophosphate (cGMP) resulting from increased activation of soluble guanylate cyclase by NO.<sup>31,32</sup> Increased cGMP would enhance the sensitivity of the photoreceptors and other neurons during dark adaptation and result in an increase of the amplitude of the dark-adapted ERG.<sup>33</sup> Furthermore, it is possible that NO also affects the ERG through S-nitrosation of proteins.<sup>28</sup> The reported effects of NO donors on the ERGs are consistent with the high bioavailable NO and increased a- and b-waves recorded from the mild diabetic rats. The effects of NOS inhibitors and NO scavengers are consistent with the low bioavailable NO and decreased a- and b-waves seen in the severe diabetic rats. Moderate diabetic rats had NO levels and ERG amplitudes that were both not significantly different from controls.

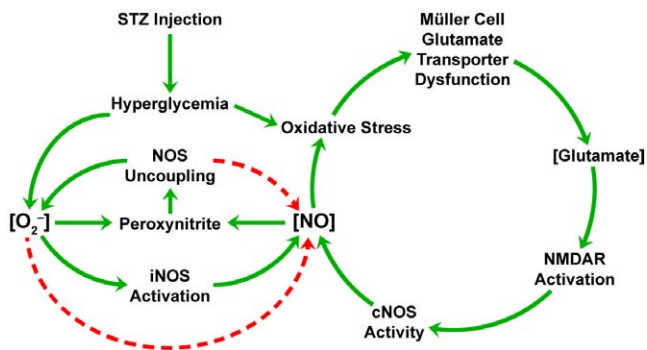


**FIGURE 6.** Proposed factors affecting NO levels in experimental DR. Green solid arrows indicate increases or upregulation, whereas red dashed arrows indicate decreases or downregulation. There is a positive feedback loop driving NO production (large green loop). Superoxide and NOS uncoupling have the effect of decreasing bioavailable NO.

Intraretinal NO concentration in diabetic rats showed a strong inverse correlation with blood glucose levels. The higher-than-control NO levels in mild diabetic rats and lower-than-control NO in severe diabetic rats suggest that other factors besides direct exposure to high glucose affects the level of bioavailable NO in the diabetic retina. This is further supported by the lack of change in NO in the acute hyperglycemic rats. There are a number of other factors that may be contributing to the observed response as mentioned above: oxidative stress, superoxide production, and peroxynitrite formation. These factors are summarized in Figure 6.

Hyperglycemia increases the intraretinal levels of radical oxygen species, glutamate, and NO.<sup>7</sup> Oxidative stress causes Müller cell glutamate transporter dysfunction early in STZ-induced diabetic rats.<sup>25</sup> The increased extracellular glutamate activates N-methyl-D-aspartate receptors and increases intracellular calcium, which can activate nNOS directly or through changes in phosphorylation of regulatory sites on the protein.<sup>34</sup> Hyperglycemia also leads to increased superoxide production, which can activate inducible NOS (iNOS).<sup>35</sup> These factors likely increase NO production in the mild diabetic rats.<sup>36,37</sup> Increased superoxide production also would lead to consumption of NO and increased formation of peroxynitrite, causing NOS uncoupling and a decrease in bioavailable NO.<sup>27</sup>

Combining these factors from the pathway seen in Figure 6 may explain the difference in NO production in the diabetic animals. The increase in bioavailability of NO in mild diabetic rats may be due to the positive feedback cycle of oxidative stress (large green loop, Fig. 6) and the decrease in bioavailability of NO in severe diabetic rats may be due to the effects of superoxide, with the moderate diabetic rats experiencing more of a balance between increased NO production and NO consumption/NOS dysfunction. Superoxide was not measured in this study, so the link between superoxide and bioavailability of intraretinal NO is speculative. However, it has been shown previously in diabetic rat retinas that high levels of superoxide consumed free NO and that the decreased bioavailability of NO leads to functional deficits even though NO production was supranormal.<sup>38</sup> Similar findings relating to superoxide decreasing the bioavailability of NO in diabetic individuals have been reported in vascular, erectile, and renal tissues.<sup>39–41</sup>

The pathway also may explain why there were no changes in the NO profiles between controls and acute hyperglycemia rats. There was likely no increase in NO because Müller cell glutamate transporter dysfunction in response to hyperglycemia takes at least 8 days to develop.<sup>42</sup> There was likely no

decrease in NO because the rats had normal amounts of antioxidants to protect against the increased superoxide levels that would otherwise consume free NO.<sup>43,44</sup> Additionally, there might not have been any changes in the acute hyperglycemia profiles because of insufficient time for iNOS to become activated, though acute hyperglycemia has been shown to increase iNOS expression after just 2 hours of exposure.<sup>45</sup> All NO measurements from the acute hyperglycemia rats were made after a minimum of 3 hours and a maximum of 5 hours after initial glucose injection; no differences were observed between early and later recordings in that period (data not shown). The experimental procedure had time limits such that the 5 hours of hyperglycemia was as long as the animal, and in vivo eyecup preparation, could be reliably maintained.

Future studies will include validation of the proposed pathway, exploration of the effects of therapeutic treatments on NO levels, and examination of NO changes over longer durations of DR. Measurement of superoxide and peroxynitrite levels would help determine if superoxide is responsible for decreasing the bioavailability of NO in severe diabetes. Antioxidant and tetrahydrobiopterin supplementation and insulin treatment will be explored as potential therapies to normalize retinal NO levels.

In conclusion, there was a strong inverse correlation between NO and blood glucose in experimental DR. Mild diabetic rats showed a higher-than-control level of bioavailable NO and severe diabetic rats showed lower-than-control levels. The vast majority of previous studies observing changes in NO in early DR have concluded that NO increases based on nitrate/nitrite measurements, which are a measure of total NO instead of bioavailable NO.<sup>9</sup> The direct measurements of NO in this study have shown that there is not a simple linear increase in bioavailable NO as the severity of diabetes increases. The data presented here may help explain the conflicting reports in the literature on NO in DR and show the importance of being able to make direct measurements of bioavailable NO in DR.

### Acknowledgments

Supported by a grant from The Macula Foundation.

Disclosure: **M.J. Guthrie**, None; **C.R. Osswald**, None; **J.J. Kang-Mieler**, None

### References

1. Doganay S, Evereklioglu C, Er H, et al. Comparison of serum NO, TNF-alpha, IL-1beta, sIL-2R, IL-6, and IL-8 levels with grades of retinopathy in patients with diabetes mellitus. *Eye*. 2002;16:163–170.
2. Ozden S, Tatlipinar S, Bicer N, et al. Basal serum nitric oxide levels in patients with type 2 diabetes mellitus and different stages of retinopathy. *Can J Ophthalmol*. 2003;38:393–396.
3. El-Remessy AB, Behzadian MA, Abou-Mohamed G, Franklin T, Caldwell RW, Caldwell RB. Experimental diabetes causes breakdown of the blood-retina barrier by a mechanism involving tyrosine nitration and increases in expression of vascular endothelial growth factor and urokinase plasminogen activator receptor. *Am J Pathol*. 2003;162:1995–2003.
4. Takeda M, Mori F, Yoshida A, et al. Constitutive nitric oxide synthase is associated with retinal vascular permeability in early diabetic rats. *Diabetologia*. 2001;44:1043–1050.
5. Leal EC, Manivannan A, Hosoya K, et al. Inducible nitric oxide synthase isoform is a key mediator of leukostasis and blood-retinal barrier breakdown in diabetic retinopathy. *Invest Ophthalmol Vis Sci*. 2007;48:5257–5265.
6. Giove TJ, Deshpande MM, Gagen CS, Eldred WD. Increased neuronal nitric oxide synthase activity in retinal neurons in early diabetic retinopathy. *Mol Vis*. 2009;15:2249–2258.

7. Kowluru R, Engerman R, Case G, Kern T. Retinal glutamate in diabetes and effect of antioxidants. *Neurochem Int.* 2001;38:385-390.
8. Kato N, Hou Y, Lu Z, et al. Kallidinogenase normalizes retinal vasopermeability in streptozotocin-induced diabetic rats: potential roles of vascular endothelial growth factor and nitric oxide. *Eur J Pharmacol.* 2009;606:187-190.
9. Patel C, Rojas M, Narayanan S, et al. Arginase as a mediator of diabetic retinopathy. *Front Immunol.* 2013;4:1-13.
10. Chen B, Keshive M, Deen W. Diffusion and reaction of nitric oxide in suspension of cell cultures. *Biophys J.* 1998;75:745-754.
11. Caldwell RB, Zhang W, Romero M, Caldwell RW. Vascular dysfunction in retinopathy: an emerging role for arginase. *Brain Res Bull.* 2010;81:303-309.
12. Eldred WD, Blute TA. Imaging of nitric oxide in the retina. *Vis Res.* 2005;45:3469-3486.
13. Toda N, Nakanishi-Toda M. Nitric oxide: ocular blood flow, glaucoma, and diabetic retinopathy. *Prog Retin Eye Res.* 2007;26:205-238.
14. Mather K, Lteif A, Steinberg H, Baron A. Interactions between endothelin and nitric oxide in the regulation of vascular tone in obesity and diabetes. *Diabetes.* 2004;53:2060-2066.
15. Hamed S, Brenner B, Aharon D, Daoud D, Roguin A. Nitric oxide and superoxide dismutase modulate endothelial progenitor cell function in type 2 diabetes mellitus. *Cardiovasc Diabetol.* 2009;8:56.
16. Guthrie MJ, Kang-Mieler JJ. Dual electroretinogram/nitric oxide carbon fiber microelectrode for direct measurement of nitric oxide in the in vivo retina. *IEEE Trans Biomed Eng.* 2014;61:611-619.
17. Runger-Brändle E, Dosso A, Leuenberger P. Glial reactivity, an early feature of diabetic retinopathy. *Invest Ophthalmol Vis Sci.* 2000;41:1971-1980.
18. Zhang X, Broderick M. Amperometric detection of nitric oxide. *Mod Asp Immunobiol.* 2000;1:160-165.
19. Schmidt K, Desch W, Klatt P, Kukovetz W, Mayer B. Release of nitric oxide donors with known half-life: a mathematical model for calculating nitric oxide concentrations in aerobic solutions. *Arch Pharmacol.* 1997;355:457-462.
20. Vielma AH, Retamal A, Schmachtenberg O. Nitric oxide signaling in the retina: what have we learned in two decades? *Brain Res.* 2012;1430:112-125.
21. Du Y, Veenstra A, Palczewski K, Kern T. Photoreceptor cells are major contributors to diabetes-induced oxidative stress and local inflammation in the retina. *Proc Natl Acad Sci U S A.* 2013;110:16586-16591.
22. Armstrong D, Al-Awadi F. Lipid peroxidation and retinopathy in streptozotocin-induced diabetes. *Free Radic Biol Med.* 1991;11:433-436.
23. Aizu Y, Oyanagi K, Hu J, Nakagawa H. Degeneration of retinal neuronal processes and pigment epithelium in the early stage of the streptozotocin-diabetic rats. *Neuropathol.* 2002;22:161-170.
24. Park SH, Park JW, Park SJ, et al. Apoptotic death of photoreceptors in the streptozotocin-induced diabetic rat retina. *Diabetologia.* 2003;46:1260-1268.
25. Li Q, Puro D. Diabetes-induced dysfunction of the glutamate transporter in retinal Müller cells. *Invest Ophthalmol Vis Sci.* 2002;43:3109-3116.
26. Alderton W, Cooper C, Knowles R. Nitric oxide synthases: structure, function, and inhibition. *Biochem J.* 2001;357:593-615.
27. Kuzkaya N, Weissmann N, Harrison D, Dikalov S. Interactions of peroxynitrite, tetrahydrobiopterin, ascorbic acid, and thiols: implications for uncoupling endothelial nitric-oxide synthase. *J Biol Chem.* 2003;278:22546-22554.
28. Vielma A, Delgado L, Elgueta C, et al. Nitric oxide amplifies the rat electroretinogram. *Exp Eye Res.* 2010;91:700-709.
29. Schmachtenberg O, Bicker G. Nitric oxide and cyclic GMP modulate photoreceptor cell responses in the visual system of the locust. *J Exp Biol.* 1999;202:13-20.
30. Ostwald P, Park S, Toledano A, Roth S. Adenosine receptor blockade and nitric oxide synthase inhibition in the retina: impact upon post-ischemic hyperemia and the electroretinogram. *Vis Res.* 1997;37:3453-3461.
31. Kurenny DE, Moroz LL, Turner RW, Sharkey KA, Barnes S. Modulation of ion channels in rod photoreceptors by nitric oxide. *Neuron.* 1994;13:215-324.
32. Djamgoz M, Sekaran S, Angotzi AR. Light-adaptive role of nitric oxide in the outer retina of lower vertebrates: a brief review. *Phil Trans R Soc Lond B.* 2000;355:1199-1203.
33. Bicker G. NO news from insect brains. *Trends Neurosci.* 1998;21:349-355.
34. Blom JJ, Giove T, Favazza TL, Akula JD, Eldred WD. Inhibition of the adrenomedullin/nitric oxide signaling pathway in early diabetic retinopathy. *J Ocul Biol Dis Inform.* 2001;4:70-82.
35. Adcock I, Brown C, Kwon O, Barnes P. Oxidative stress induces NFκB DNA binding and inducible NOS mRNA in human epithelial cells. *Biochem Biophys Res Comm.* 1994;199:1518-1524.
36. Chiang HT, Cheng WH, Lu PJ, et al. Neuronal nitric oxide synthase activation is involved in insulin-mediated cardiovascular effects in the nucleus tractus solitarius of rats. *Neurosci.* 2009;159:727-734.
37. Toba H, Gomyo E, Miki S, et al. Hyperinsulinemia increases the gene expression of endothelial nitric oxide synthase and the phosphatidylinositol 3-kinase pathway in rat aorta. *Clin Exp Pharmacol Physiol.* 2006;33:440-447.
38. Schaefer S, Kajimura M, Tsuyama S, et al. Aberrant utilization of nitric oxide and regulation of soluble guanylate cyclase in rat diabetic retinopathy. *Antioxid Redox Signal.* 2003;5:457-465.
39. Mason RP, Kalinowski L, Jacob R, et al. Nebivolol reduces nitroxidative stress and restores nitric oxide bioavailability in endothelium of black Americans. *Circulation.* 2005;112:3795-3801.
40. Ishii K, Patel K, Lane P, et al. Nitric oxide synthesis and oxidative stress in the renal cortex of rats with diabetes mellitus. *J Am Soc Nephrol.* 2001;12:1630-1639.
41. Bivalacqua T, Mustafa U, Kendirci M, et al. Superoxide anion production in the rat penis impairs erectile function in diabetes: influence of in vivo extracellular superoxide dismutase gene therapy. *J Sex Med.* 2005;2:187-198.
42. Mysona B, Dun Y, Duplantier J, Ganapathy V, Smith S. Effects of hyperglycemia and oxidative stress on the glutamate transporters GLAST and system x<sub>c</sub><sup>-</sup> in mouse retinal Müller glial cells. *Cell Tissue Res.* 2009;335:477-488.
43. Nishida T, Nakagawa S, Manabe R. Superoxide dismutase activity in the diabetic rat retina. *Jpn J Ophthalmol.* 1984;28:377-382.
44. Kanwar M, Chan PS, Kern T, Kowluru R. Oxidative damage in the retinal mitochondria of diabetic mice: possible protection by superoxide dismutase. *Invest Ophthalmol Vis Sci.* 2007;48:3805-3811.
45. Ceriello A, Quagliaro L, D'Amico M, et al. Acute hyperglycemia induces nitrotyrosine formation and apoptosis in perfused heart from rat. *Diabetes.* 2002;51:1076-1082.